

# Particle lofting from substrate exposed to plasma and electron beam

P. V. Krainov,<sup>1,2, a)</sup> V. V. Ivanov,<sup>1</sup> D. I. Astakhov,<sup>1,3</sup> V. V. Medvedev,<sup>1,2</sup> V. V. Kvon,<sup>4</sup> A. M. Yakunin,<sup>4</sup> and M. A. van de Kerkhof<sup>4</sup>

<sup>1)</sup> *Institute for Spectroscopy of the Russian Academy of Sciences, Fizicheskaya str. 5, Troitsk, Moscow 108840, Russia*

<sup>2)</sup> *Moscow Institute of Physics and Technology, Institutskiy pereulok str. 9, Dolgoprudny, Moscow region 141701, Russia*

<sup>3)</sup> *ISTEQ B.V., High Tech Campus 9, 5656 AE Eindhoven, The Netherlands*

<sup>4)</sup> *ASML Netherlands B.V., De Run 6501, 5504DR Veldhoven, The Netherlands*

(Dated: October 10, 2021)

A nanometer-sized dielectric particle lying on a dielectric substrate is exposed to the flux of low-energy electrons, ion and electron fluxes from a cold plasma and the fluxes from the combination of these two sources with the help of particle-in-cell simulation to investigate the particle lofting phenomenon. The results are of interest for dust mitigation in the semiconductor industry, the lunar exploration, and the explanation of the dust levitation.

## I. INTRODUCTION

EUVL scanners<sup>1</sup> operate in a low-pressure hydrogen atmosphere<sup>2</sup>. The propagation of ionizing EUV radiation in this atmosphere inevitably leads to the formation of hydrogen plasma. In turn, this plasma interacts with the walls of the scanner chamber and with various functional surfaces. In this case, exposure to plasma can lead to the release of pollution particles from such surfaces and their further transport to the sensitive surfaces of the mask and wafer<sup>3,4</sup>. Controlling and minimizing particle contamination requires detailed investigation of the particle release mechanisms.

Experimental and theoretical studies of the release of particles from surfaces under the influence of plasma have been carried out since the early 1990s. These studies were aimed at interpreting the observation of levitation of dust particles over the surface of airless space bodies such as the Moon or asteroids. Experimental studies were carried out mainly using micron-sized regolith particles. Nonetheless, these published results allow the theoretical particle release models to be tested and validated.

Several experimental groups detected the most intense particle release by simultaneous exposure to low-temperature plasma and low-energy electron beam<sup>5–7</sup>. Besides, some of them detected release of dust particles exposed to only electron beam<sup>7</sup>. In the recent work<sup>8</sup> we studied lofting by electron beam with the help of particle-in-cell numerical simulation. We found that interaction between charges accumulated on surfaces of particle and substrate can be the reason of lofting. This finding is in agreement with the recently developed "patched charge model"<sup>7,9</sup> but in contrast to the widespread hypothesis<sup>6,10</sup> that explains particles transport by interaction with the electric field of plasma sheath.

In this work we apply our particle-in-cell model<sup>11</sup> for

further investigation of the lofting phenomenon. We carried out a simulation of nanometer-sized dielectric particle lofting resting on a dielectric substrate in a chamber filled by hydrogen and exposed to low-energy electron beam. By varying hydrogen pressure, we investigated a range of conditions from a pure electron beam to a low-temperature plasma including their combination. We found that a plasma addition to an electron beam increases repulsive force and can make particle lofting possible from a dielectric substrate as thin as a naturally formed oxide layer.

The simulation consists of two stages. The first stage described in sec. III is the simulation of a plasma formation in a chamber filled by hydrogen and induced by an electron beam. The second stage described in sec. IV is the simulation of a particle charge buildup under the exposure of ions and electrons from plasma.

## II. FORCES

The object of our study is a dielectric particle lying on a dielectric surface. The particle experiences the action of five forces. Two repulsive electrostatic forces: the interaction with an external electric field (e.g., field of plasma sheath) and the interaction between charges on the particle surface and charges on the substrate surface, two attractive forces: a surface adhesive force and the interaction of the particle charge with its electric image in the dielectric substrate (mirror force), and gravitational force.

It was concluded previously in several papers<sup>5,6,8</sup> that gravitational force is several orders lower than adhesive van der Waals force. Therefore, there are only four forces to be considered.

As a major surface adhesive force the van der Waals force is considered. In spite of the availability of the Hamaker theory and several more comprehensive theories<sup>12</sup> for estimation of van der Waals force, its value is not a well defined. A literature review gives a range from  $10^{-12}$  to  $10^{-8}$  N for 100 nm particle.

<sup>a)</sup> Electronic mail: [pavel.krainov@phystech.edu](mailto:pavel.krainov@phystech.edu)

The lower limit of this range requires  $n \cdot E \geq 10^7 \text{ V m}^{-1}$ , where  $n = |Q/e|$  is the number of charges collected by the particle and  $E$  is the electric field. This requires a supercharge of particle or extremely large value of electric field, that is not reached in a plasma used in any conducted experiment about particle lofting.

Recently we demonstrated that other two forces is of great importance for particle lofting in case of exposure to low-energy electric beam. The calculation of other two forces in case of exposure to plasma and electron beam is the issue discussed in this article.

### III. SIMULATION OF PLASMA FORMATION

The simulation of plasma formation was conducted with the help of a two-dimensional cylindrically symmetrical particle-in-cell (PIC) model<sup>11</sup>, that follows the general PIC scheme<sup>13</sup>. At every time step ions and electrons represented by super particles update their positions and velocities in accordance with electric field distribution. Then, a Poisson equation solver is used to obtain a new electric field distribution corresponding to the distribution of ions and electrons. A Monte-Carlo (MC) scheme was used to introduce collisions of electrons, ions and fast neutrals with molecules from the background gas<sup>11</sup>. Electron-electron, electron-ion, ion-ion Coulomb collisions as well as three body collision were neglected, because of low probability due to low plasma density (fig. 2). The model was previously validated in experiments with extreme ultraviolet induced hydrogen plasma<sup>14–16</sup>.

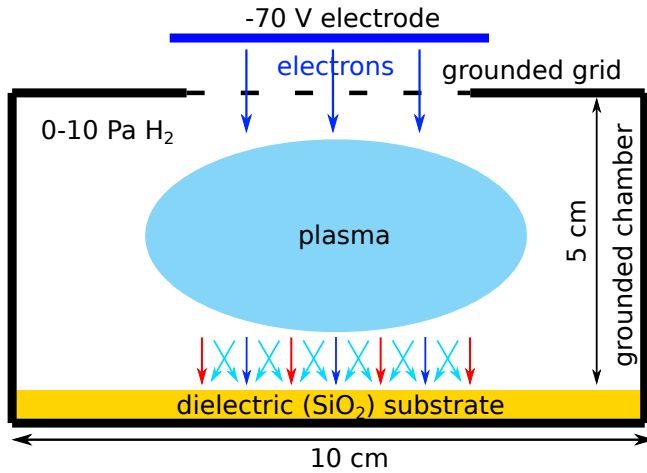


Figure 1. The setup that was simulated to obtain ion and electron fluxes to the substrate.

The setup shown in fig. 1 was simulated to obtain ion and electron fluxes and spectra. This setup mimics setups used in the real experiments<sup>5–7</sup>. A 5 cm high and 10 cm in diameter cylindrical metallic chamber with grounded walls was filled by hydrogen with pressure from 0 to 10 Pa. The bottom wall of the chamber was cov-

ered by a silicon dioxide substrate. A 3 cm in diameter grounded grid was set in the center of the top wall. The grid transparency was 75%. An electrode placed in front of the grid emitted  $2 \cdot 10^{13} \text{ cm}^{-2} \text{ s}^{-1}$  electrons. The potential applied to this electrode (-70 V) pushed these electrons inside the chamber. The electrons ionized hydrogen and caused plasma formation. The resolution of computational mesh was chosen to resolve the Debye length.

The simulation lasted until density and potential of the plasma in the center of the chamber and substrate potential reached a stationary value. It took about several milliseconds of simulation internal time. The dependencies of plasma density and fluxes to the substrate on hydrogen pressure are shown in fig. 2. Stationary values are given. Our model takes into account secondary electron emission (see description in sec. IV). The electron flux plotted in fig. 2 includes only incoming electrons and does not include outgoing secondary electrons. The last is the reason of the difference between stationary electron and ion fluxes in fig. 2.

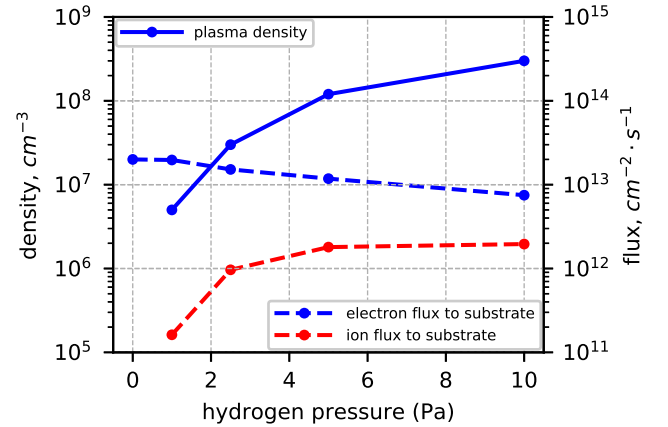


Figure 2. The dependencies of plasma density and fluxes to the substrate on hydrogen pressure.

Energy distribution functions of electron flux to the substrate at different pressure are demonstrated in figs. 3. Every spectrum consists of two main components: 70 eV electron injected in the chamber and low-energy electrons of the formed plasma. The peak of 70 eV electrons decreases with hydrogen pressure, because more electrons interacts with the background gas molecules. The shift of the right edge of the spectra with hydrogen pressure is caused by different stationary potential of the dielectric substrate at different gas pressure. It varies from -2.5 V to -0.5 V. The average energy of electron flux reduces from 70 eV for 0 Pa to about 20 eV for 10 Pa of the background gas pressure.

Collisions between electrons and gas molecules produces  $H_2^+$  ions, that converts in  $H_3^+$  ion in collisions with gas molecules within several microseconds. Hence,  $H_3^+$  is the main ion of the plasma. Spectra of  $H_3^+$  flux to the substrate at different gas pressures are given in fig. 4. The energy of spectrum maximum equals to the plasma

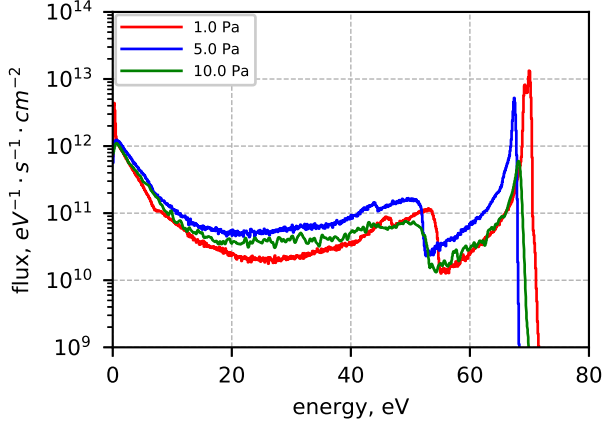


Figure 3. Spectra of electron flux to the substrate at different hydrogen pressures.

sheath voltage as well as for electrons and varies with the background gas pressure.

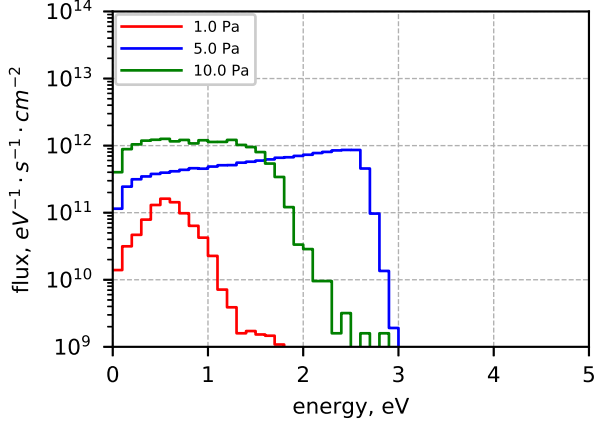


Figure 4. Spectra of ion flux to the substrate at different hydrogen pressures.

#### IV. SIMULATION OF PARTICLE CHARGE BUILDUP

Ion and electron fluxes obtained at the first stage of the simulation were used to expose a dielectric particle resting on a dielectric substrate to calculate the force. This simulation follows the idea of the simulation we performed earlier<sup>8</sup> for an electron beam. A brief description is given below. A 100 nm dielectric particles was placed 1 nm above a dielectric substrate. Two dielectric substrate of different thickness were used: thick (2000 nm) and thin (3 nm). Ions and electrons bombarded the particle and the substrate.

The dielectric substrate rested on a grounded electrode, that was the bottom boundary of the simulation domain. The other boundaries were several micrometers away from the particle as the field of the charged particle

is negligible at such a distance. The top boundary was a biased electrode. Its potential was equal to the potential of the dielectric substrate from the first stage. The side boundary was set to be a mirror. It imitated the rest of the charged dielectric substrate. A non-uniform rectangular grid was used in the simulation. Its maximum resolution was equal to 1 nm to resolve the distance between the particle and the substrate.

The material of the dielectric we used is silicon dioxide ( $SiO_2$ ). We took into account dielectric permittivity ( $\epsilon = 3.9$ ), electron induced secondary electron emission yield<sup>17</sup>, the spectrum<sup>18</sup> and angular distribution<sup>19</sup> of secondary electron emission. The dielectric was assumed to be an ideal insulator.

The simulation lasted until the distribution of charges over the particle and the substrate surfaces reached a stationary state. The distributions obtained in the simulations at two hydrogen pressures (0 and 2.5 Pa) are given in fig. 5. The typical force dynamics obtained in case of simultaneous exposure to electron beam and plasma is given in fig. 6.

The left distribution in fig. 5 corresponds to the exposure to an electron beam only. The lower part of the particle accumulates secondary electrons emitted by nearby region of the substrate due to secondary electron emission. This simulation was described previously in detail<sup>8</sup>. In case of plasma addition (the right distribution in fig. 5), the negatively charged lower part of the particle attracts slow ions (their energy is about several eV) pulls them in in the gap between the particle and the substrate. This reason causes the formation of positively charged regions on the substrate and the particle in the place of contact. In other words, the negatively charged particle acts as a focusing lens for ions. In case of plasma addition, the upper part of the particle is charged positively too. It directly experiences the bombardment of ions. Besides, it experiences the bombardment of electron with energy larger than the first crossover energy for silicon dioxide. Secondary electron emission yield is more than 1 for such electrons, i.e. in average such electrons leave a positive charge on a dielectric after collision.

Fig. 6 demonstrates the result of the simulation for 2.5 Pa of hydrogen pressure. The force shown includes both electrostatic components: the repulsive interaction between charges accumulated on the substrate and the particle and the mirror force. The force was calculated as integral over particle of product of electric field and charge density.

A charge distribution over surfaces obtained in a simulation is fluctuating. Our 2-D PIC model can not calculate properly the force fluctuation caused by fluctuation of charge distribution due to the axial symmetry of the model. That is why a charge distribution was smoothed at the stage of postprocessing to take into consideration the "macro" effects of electron and ion accumulation. We used Savitzky-Golay filter to approximate the integral with variable upper limit over the particle and the substrate surface. The order of the filter was

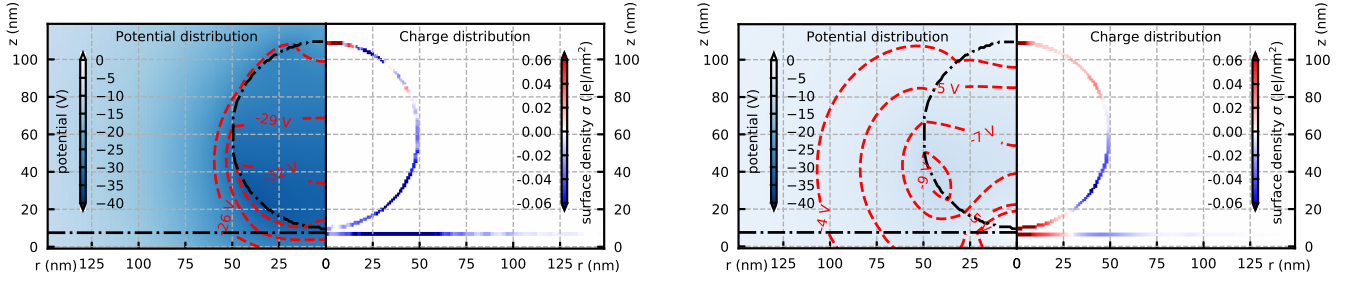


Figure 5. Distribution of accumulated charges over the particle and substrate surfaces for two values of hydrogen pressure: 0 Pa (left) and 2.5 Pa (right).

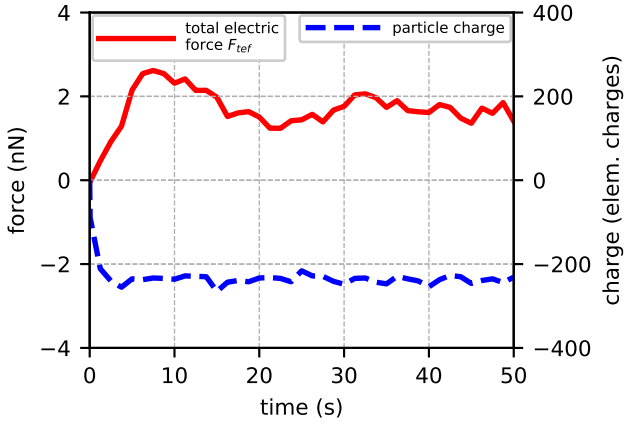


Figure 6. Dynamics of the particle charge and the electrostatic force acting on the particle in case of 2.5 Pa of hydrogen pressure.

equal to 3, because the function to be approximated has 2 extremum points. The width of the filter was equal to one third of the corresponding coordinate (radius for the substrate and azimuthal angle for the particle) range. The last thing to be noted is that fig. 5 gives smoothed distributions. Dynamics of the force and the charge at other pressures is the same as in case of 2.5 Pa hydrogen pressure.

Stationary values of the force acting on the dielectric particle and the particle charge for different hydrogen pressures are given in fig. 7. The most interesting feature of this plot is the transition from 0 Pa to 2.5 Pa, i.e., plasma addition. According to the conducted simulation, it is possible to take off a particle from a thick dielectric substrate with the help of a low-energy electron beam, but it is not possible in case of thin dielectric. The plasma addition helps to cope with this problem. This can be explained by two reasons. Ion accumulation under the particle gives a significant contribution to the repulsion between the particle and the substrate. Plasma addition

results to lower total particle charge, that decreases the mirror force.

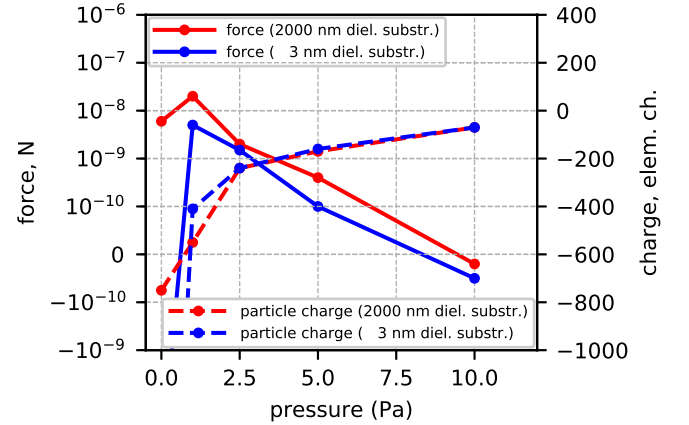


Figure 7. Dependency of the force acting on the particle and the particle charge obtained in the simulations with two substrates of different thickness.

## V. DISCUSSION

Table I demonstrates a qualitative agreement between the results of our simulation and the published experiments. To simulate a particle exposure to only plasma we exploited the same setup. We registered ion and electron fluxes to the dielectric substrate in the region, that was not directly exposed to 70 eV electrons.

## VI. CONCLUSION

The authors investigated a 100 nm silicon dioxide particle resting on a silicon dioxide substrate. With the help of particle-in-cell numerical model, we exposed the particle to the flux of a low-energy electron beam, electron

Table I. Qualitative comparison of the simulation results with the experimental results. "+" sign means detected particle lofting, "-" sign means that particle lofting was not observed. The number in parentheses is  $l/\lambda$ , where  $l$  is the height of the simulated setup (at the first stage),  $\lambda$  is the mean free path of an electron in hydrogen before ionization collision. This value reflects the portion of electrons absorbed by hydrogen and turned into plasma

		electron beam		electron beam + plasma			plasma (out of beam)	
		0 Pa (0)	1 Pa (0.1)	2.5 Pa (0.25)	5 Pa (0.5)	10 Pa (1.0)	1 Pa	10 Pa
simulation	thick (2000 nm)	+	+	+	+	-	-	-
	thin (3 nm)	-	+	+	-	-	-	-
		e beam		e beam + plasma			plasma	
experiment	Flanagan <sup>6</sup> (thick diel.)	-		+ (0.05)			-	
	Sheridan <sup>5</sup> (thick diel.)	-		+ (0.1)			-	
	Wang <sup>7</sup> (partilces heap)	+		+ (0.1)			-	

and ion fluxes of cold plasma and fluxes from the combination of these two sources. We found that a plasma addition to an electron beam results to the ion accumulation between the substrate and the particle. As a result, this plasma addition increases the force acting on the particle and make particle lofting possible from the substrate as thin as a naturally formed oxide layer. The simulation results are in qualitative agreement with the published experiments.

## REFERENCES

- <sup>1</sup>M. A. van de Kerkhof, J. P. H. Benschop, and V. Y. Banine, *Solid-State Electronics Selected Papers from the Future Trends in Microelectronics (FIM-2018) Workshop*, **155**, 20 (2019).
- <sup>2</sup>J. Beckers, T. van de Ven, R. van der Horst, D. Astakhov, and V. Banine, *Applied Sciences* **9**, 2827 (2019).
- <sup>3</sup>M. van de Kerkhof, T. van Empel, M. Lercel, C. Smeets, F. van de Wetering, A. Nikipelov, C. Cloin, A. Yakunin, and V. Banine, in *Extreme Ultraviolet (EUV) Lithography X*, Vol. 10957 (International Society for Optics and Photonics, 2019) p. 109570U.
- <sup>4</sup>L. Scaccabarozzi, N. A. Lammers, R. Moors, and V. Banine, *Journal of Adhesion Science and Technology* **23**, 1603 (2009).
- <sup>5</sup>T. E. Sheridan, J. Goree, Y. T. Chiu, R. L. Rairden, and J. A. Kiessling, *Journal of Geophysical Research: Space Physics* **97**, 2935 (1992).
- <sup>6</sup>T. M. Flanagan and J. Goree, *Physics of Plasmas* **13**, 123504 (2006).
- <sup>7</sup>X. Wang, J. Schwan, H.-W. Hsu, E. Grün, and M. Horányi, *Geophysical Research Letters* **43**, 6103 (2016).
- <sup>8</sup>P. V. Krainov, V. V. Ivanov, D. I. Astakhov, V. V. Medvedev, V. V. Kvon, A. M. Yakunin, and M. A. van de Kerkhof, *Plasma Sources Science and Technology* **29**, 085013 (2020).
- <sup>9</sup>J. Schwan, X. Wang, H.-W. Hsu, E. Grün, and M. Horányi, *Geophysical Research Letters* **44**, 3059 (2017).
- <sup>10</sup>T. E. Sheridan and A. Hayes, *Applied Physics Letters* **98**, 091501 (2011).
- <sup>11</sup>D. Astakhov, *Numerical Study of Extreme-Ultra-Violet Generated Plasmas in Hydrogen*, PhD Thesis, University of Twente, Enschede (2016).
- <sup>12</sup>C. Q. LaMarche, S. Leadley, P. Liu, K. M. Kellogg, and C. M. Hrenya, *Chemical Engineering Science* **158**, 140 (2017).
- <sup>13</sup>C. K. Birdsall and A. B. Langdon, *Plasma Physics via Computer Simulation*, Series in Plasma Physics (Taylor & Francis, 1991).
- <sup>14</sup>D. I. Astakhov, W. J. Goedheer, C. J. Lee, V. V. Ivanov, V. M. Krivtsun, A. I. Zotovich, S. M. Zyryanov, D. V. Lopaev, and F. Bijkerk, *Plasma Sources Science and Technology* **24**, 055018 (2015).
- <sup>15</sup>D. I. Astakhov, W. J. Goedheer, C. J. Lee, V. V. Ivanov, V. M. Krivtsun, K. N. Koshelev, D. V. Lopaev, R. M. van der Horst, J. Beckers, E. A. Osorio, and F. Bijkerk, *Journal of Physics D: Applied Physics* **49**, 295204 (2016).
- <sup>16</sup>A. Abrikosov, V. Reshetnyak, D. Astakhov, A. Dolgov, O. Yakushev, D. Lopaev, and V. Krivtsun, *Plasma Sources Science and Technology* **26**, 045011 (2017).
- <sup>17</sup>A. Dunaevsky, Y. Raites, and N. J. Fisch, *Physics of Plasmas* **10**, 2574 (2003).
- <sup>18</sup>E. Schreiber and H. J. Fitting, *Journal of Electron Spectroscopy and Related Phenomena* **124**, 25 (2002).
- <sup>19</sup>N. Bundaleski, M. Belhaj, T. Gineste, and O. M. N. D. Teodoro, *Vacuum 13th European Vacuum Conference Joint Meeting with 7th European*